OPEN

EXPERIMENTAL

Morphometric and Functional Analysis of Axonal Regeneration after End-to-end and End-to-side Neurorrhaphy in Rats

Carlos Eduardo Fagotti de Almeida, MD, PhD*
Jayme Adriano Farina Junior, MD, PhD*
Benedicto Oscar Colli, MD, PhD†

Background: End-to-side neurorrhaphy is controversial in the literature and has sparked debate over its degree of recovery. In this study, nerve regeneration was assessed in rats after end-to-side neurorrhaphy by morphometric analysis, electromyography, electron microscopy, and retrograde horseradish peroxidase (HRP) and Fluoro-Gold (FG; Fluorochrome Inc., Denver, Colo.) transport and then compared to end-to-end neurorrhaphy and sham operation.

Methods: Thirty-seven animals were operated on and divided randomly into 4 groups: group 1, sham; group 2, end-to-end neurorrhaphy; group 3, end-to-side neurorrhaphy with an epineural window; and group 4, end-to-side neurorrhaphy without an epineural window. Three months after surgery, HRP was injected into the peroneal muscles. After 48 hours, nerve segments and lumbar spine segments were collected. Electromyography data were compared between groups, and FG uptake was compared in 20 other animals. Analysis of variance with Tukey-Kramer correction was used for group comparison.

Results: The fiber count after end-to-end neurorrhaphy was higher than after end-to-side neurorrhaphy with an epineural window ($q = 5.243$ and $P < 0.01$) or without an epineural window ($q = 4.951$ and $P < 0.01$). HRP labeling showed a difference between group 2 and end-to-side neurorrhaphy with an epineural window ($q = 5.291$ and $P < 0.01$) and without an epineural window ($q = 5.617$ and $P < 0.01$). There was also a difference in mean area labeled with FG. Furthermore, the amplitudes of the action potentials were significantly higher in groups 1 and 2.

Conclusions: There was nerve regeneration in all groups studied. However, the end-to-end neurorrhaphy group had better reinnervation than the end-to-side neurorrhaphy groups. *(Plast Reconstr Surg Glob Open 2015;3:e326; doi: 10.1097/GOX.0000000000000280; Published online 17 March 2015.)*

*From the *Division of Plastic Surgery, Department of Surgery and Anatomy, Ribeirão Preto Medical School, University of São Paulo, São Paulo, Brazil; and †Division of Neurosurgery, Department of Surgery, Ribeirão Preto Medical School, University of São Paulo, São Paulo, Brazil.*

Received for publication March 9, 2014; accepted January 7, 2015.

DOI: 10.1097/GOX.0000000000000280

Nerve regeneration is considered to be a highly complex phenomenon resulting from a cascade of events aiming at the preparation of the microenvironment of the injured nerve for directed axonal growth.

Disclosure: *The authors have no financial interest to declare in relation to the content of this article. This study was supported by FAPESP. The Article Processing Charge was paid for by the authors.*

Supplemental digital content is available for this article. Clickable URL citations appear in the text.

End-to-end neurorrhaphy and autograft nerve repairs are universally accepted. However, the end-to-side neurorrhaphy is controversial in the literature, leading to discussion on the axonal growth and the degree of motor and sensory recovery.

In the present investigation, nerve regeneration was studied in rats by morphometric analysis, electroneuromyography, electron microscopy, and retrograde horseradish peroxidase (HRP) and Fluoro-Gold (FG) uptake after end-to-end and end-to-side neurorrhaphy with and without an epineural window.

Kristensson and Olsson,[1] in 1971, using HRP as a neurotracer, unequivocally demonstrated a neural connection by identifying retrograde HRP transport after intramuscular HRP injection. Later, Schmued and Fallon[2] described FG as a new dye for retrograde axonal transport and reported its properties of intense fluorescence and resistance to extinction.

The concept of end-to-side neurorrhaphy without opening the epineurium was described by Viterbo et al.[3] In their experiment on rats, the distal stump of the recipient nerve was coupled to the lateral surface of the donor nerve, and morphological and electrophysiological observations revealed the presence of regenerated myelin fibers. The myelin sheath was no impediment for axonal growth. In another study, using the same animal model but with the removal of an epineurial window, axonal growth was observed from the donor to the recipient nerve both morphologically and electrophysiologically, with no damage to the donor nerve.[4,5] This fact provoked skepticism because it is known that the axon cannot cross the layers wrapped around the nerve.

Suspected lateral axonal budding in an uninjured donor nerve 4 weeks after end-to-side neurorrhaphy with an epineurial window was reported by Terzis et al.[6]

In a clinical study, other authors did not observe clinical, electrophysiological, or histological recovery in patients subjected to end-to-side repairs.[7] Recovery was only detected in fascicle transfer. The authors did not recommend this procedure in clinical practice, stating that the conjunctival layer of the peripheral nerve represents a barrier against the penetration of regenerating axons.

The objectives of the present study were (1) to assess the regeneration of the fibular nerve after end-to-end and end-to-side neurorrhaphies with and without an epineurial window in rats by determining HRP and FG propagation from the axonal end to the motor neurons of the ventral horn of the spinal cord; morphometric analysis (count of the number of regenerated nerve fibers); electron microscopy (perimeter of the fiber and axon); and electromyography (amplitude and latency) and (2) to compare HRP and FG uptake after end-to-side neurorrhaphy and after end-to-end neurorrhaphy.

METHODS

An experimental, randomized, prospective study was conducted on adult male Wistar rats weighing 220–300 g from the Central Animal House of the Ribeirão Preto Medical School of University of São Paulo.

The animals were allowed to adapt to the facilities for a period of 48 hours before the beginning of the experiment and then divided at random into 4 groups of 10 animals into the following experimental groups by drawing lots, with no type of restriction: group 1, sham (no nerve section): surgical exploration of the fibular nerve without sectioning; group 2, end-to-end neurorrhaphy; group 3, end-to-side neurorrhaphy with an epineurial window: in this group, the animals were submitted to end-to-side neurorrhaphy between the distal stump of the fibular nerve sectioned at 5 mm from its emergence and the lateral surface of the tibial nerve, with an epineurial window, using a microsurgical technique; and group 4, end-to-side neurorrhaphy, without an epineurial window: the same surgical procedure as for group 3 animals but without an epineurial window.

Surgery

The animals were anesthetized intraperitoneally with 10% ketamine (0.1 ml/100 g body weight) and 10% xylazine (0.05 ml/100 g body weight) and positioned in surgical decubitus on a surgical board, and the skin of the posterior region of the thigh was shaved. Next, a 3-cm-long skin incision was performed on the posterolateral side of the right thigh to the popliteal fossa. The fascia was pulled apart between the femoris biceps and semimembranosus muscles, with exposure of the sciatic nerve and of its 3 branches—common fibular, tibial, and sural nerves—in the popliteal fossa. Then, the fibular and tibial nerves were dissected with the aid of a microscope (×16 magnification) using a microsurgical technique. At this point, the animals were assigned at random (drawing lots) to their groups, with no type of restriction:

Group 1 (sham): The fibular nerves were isolated and exposed for 30 minutes (the time estimated for suture in the other groups). In the animals assigned to groups 2, 3, and 4, the fibular nerves were sectioned and manipulated as shown below.

Group 2 (end-to-end neurorrhaphy): The fibular nerves were submitted to end-to-end repair using a microsurgical technique.

Group 3 (end-to-side neurorrhaphy with an epineurial window): The distal stumps of the fibular nerves were sutured to the intact tibial nerve by end-to-side neurorrhaphy after a 1-mm window was cut in the epineurium using mononylon 11.0 sutures (Ethicon; Johnson & Johnson, São Paulo, Brazil). The proximal stumps were buried in the adjacent musculature with 8-0 nylon.

Group 4 (end-to-side neurorrhaphy without an epineurial window): In this group, the procedure was the same as in group 3, except for the absence of an epineurial window.

Nerve Removal

Three animals died during the late postoperative period, that is, 3 months after surgery. Thirty-seven animals were again anesthetized intraperitoneally with ketamine and xylazine. An incision was made over the initial scar, the muscles were pulled apart, and the fibular and tibial nerves were identified.

In the animals submitted to end-to-end neurorrhaphy, 3 segments of the fibular nerve were collected—proximal to the nerve anastomosis, in the suture region, and distal to the anastomosis—for morphometric study.

In the animals submitted to end-to-side neurorrhaphy with or without an epineurial window, 4 nerve segments were collected: 2 transverse segments of the tibial nerve (before and after end-to-side neurorrhaphy), 1 in the region of the end-to-side anastomosis between the tibial and fibular nerves (in the longitudinal direction), and 1 in the distal stump of the fibular nerve.

Only one segment of the fibular nerve was obtained from the animals submitted to the sham procedure.

Nerve Processing

The material obtained was fixed in 2.5% glutaraldehyde for 2 hours, immersed in 0.1 M phosphate buffer, postfixed in 1% osmium tetroxide, dehydrated in increasing ethanol concentrations, and embedded in Araldite 6500 resin (St Louis, Miss.). Crosswise 0.5-µm-thick sections were then cut, mounted on histological slides, stained with 1% toluidine blue, and coverslipped.

Fiber Digitization

Images were digitized with an Axiophot II (Carl Zeiss, Jena, Germany) microscope using a JVC video camera (TK 1270; JVC USA, Wayne, N.J.), a motor-driven platen coupled to the microscope, and a KS 400 app (Kontron 2.0; Eching Bei, Munich, Germany).

Images of the nerve were captured inside the window area. These labeled structures were transformed to a black and white binary image for automatic identification by the software. However, "binarization" failed to eliminate all irregularities, and a manual adjustment was necessary. After image adjustment, myelin fibers were counted.

Electron Microscopy

The prepared materials were then cut into 700-Å-thick sections with an ultramicrotome in a liquid medium. The sections were placed on copper grids, dried, and contrasted with uranyl acetate for 25 minutes, washed with twice-distilled water, immersed in lead citrate for 3 minutes, washed again, and then dried at room temperature.

The sections were analyzed with a transmission electron microscope at ×5000, ×40,000, and ×100,000 magnification. Next, the perimeters of the fiber and of the axon on each grid were calculated, and the thickness of the myelin sheath was determined. The perimeter was calculated using the freehand selection tool of the Mac Biophotonics ImageJ computer software (Bethesda, Md.), and myelin thickness was determined using the straight line selection tool. After image selection, the measurement option of the software was used, and the data were exported to an Excel (Microsoft, São Paulo, Brazil) spreadsheet.

Removal of the Spinal Cord

Before removal of the nerve fragments and of the spinal cord, 10 µl free 20% HRP was injected with a Hamilton syringe (Hamilton Company, Franklin, Mass.) under direct view into the fibular muscles of the lower limbs of all animals studied.

Two days after HRP injection into the fibular muscle and after collection of the nerve segments, 32 animals were submitted to thoracotomy. An orifice was opened with a scissors in the left ventricle, a catheter was inserted, and the infusion pump was started. The animals were slowly perfused through the heart with saline solution (0.05 M phosphate-buffered saline) at room temperature over a period of 30 minutes. Next, they were slowly perfused with a fixative solution consisting of 4% paraformaldehyde and 2.5% glutaraldehyde dissolved in 0.1 M phosphate buffer (one third of each product) for 30 to 45 minutes.

At the end of perfusion, laminectomy was performed. The muscles inserted in the spinous processes were pulled apart, and the laminae were removed with a micropunch, preserving the dura mater. The spinal cord was sectioned after visualization of the L3, L4, L5, and L6 roots up to their entry in the cord (Fig. 1). The cord segment was placed in a vessel containing 4% paraformaldehyde for 30 minutes and then in a 20% saccharose solution for 2 hours for tissue cryoprotection. The

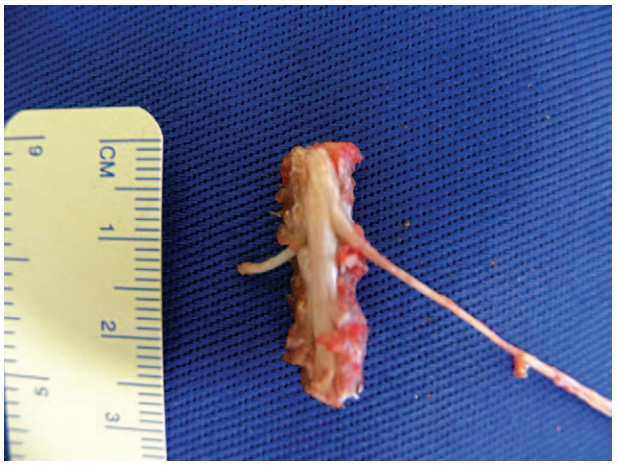

Fig. 1. Removal of spinal cord. The right side of the cord has the nerve segment with greater length.

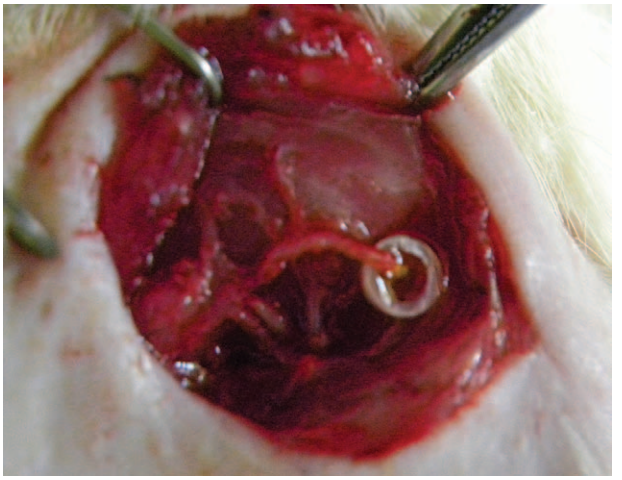

Fig. 2. Peroneal nerve inside the capsule with FG.

segment was then placed on a support with Tissuetek (Tissue-Tek O.C.T. Compound; Sakura Finetek, Alphen aan den Rijn, The Netherlands) inside a beaker containing isopentane and frozen in liquid nitrogen.

Processing of HRP-labeled Spinal Cord Fragments

Once cryoprotected, the spinal cord samples were cut into 30-µm-thick sections in a cryostat at −18°C with an 8° angulation and then transferred to DAB in a dark chamber for 20 minutes under manual shaking. After this period, the diaminobenzidine reaction was blocked with phosphate-buffered saline and the material was washed in running water.

An Axio Scope A1 light field microscope (Zeiss) and a filter with BP 510–560, FT 580, and LP 590 were used for HRP visualization in the anterior horn of the spinal cord.

HRP-labeled images in the anterior horn of the spinal cord were processed with the ImageJ software. The images at ×10 magnification were marked and selected in gray tones with a calibration limit between 20 and 34. After image selection, the Analyze and Measure options of the software were used and the data were exported to an Excel spreadsheet.

Removal of the Spinal Cord after FG Labeling

Twenty additional animals were divided at random into 4 groups ($N = 5$ each), respectively, submitted to end-to-end neurorrhaphy, end-to-side neurorrhaphy with an epineurial window, end-to-side neurorrhaphy without an epineurial window, and sham operation.

Four months after the surgical procedure, the animals were reoperated on and anesthetized as mentioned above for exposure of the fibular nerve. The fibular nerve was immersed in a capsule containing FG for 60 minutes (Fig. 2).

Five days after exposure to the dye, the animals were again anesthetized and submitted to cardiac perfusion. Spinal cord fragments were frozen and cut into 30-µm-thick sections with a cryostat, and the sections were mounted on slides, covered, and allowed to dry in a refrigerator for 12 hours.

FG labeling of motor neurons was visualized with an Axio Scope A1 fluorescence microscope using the ImageJ software. The desired area was marked with calibration limits of 130–140. The filter showed BP 340–380, FT 400 excitation, and an LP barrier (emission wavelength) of 430, thus lighting in blue and capturing in green.

Electrophysiological Test

The electrophysiological test was carried out under anesthesia before collection of the material. Nerve conduction was performed by electrical stimulation of the fibular nerve, and the evoked response was recorded at a distance. The parameters assessed were amplitude and latency, with the needle electrodes implanted in the percutaneous fibular muscles and the reference electrodes implanted distally to the neurorrhaphies. The action potentials of the motor unit were analyzed during contraction.

Data Analysis

Because group data were numerical and continuous, the arithmetic means were compared by analysis of variance (ANOVA). The Kolmogorov-Smirnov test revealed that the data for all groups showed normal distribution. The Bartlett test was used to determine the difference between standard deviations.

The F test statistic was then used to determine the ratio of the mean squares between groups and the

ratio of the mean squares within groups according to the appropriate degrees of freedom. The Tukey-Kramer test was used to determine group differences.

Linear Regression

Linear regression was used to predict the number of fibers of the fibular nerve based on neuronal HRP labeling in the anterior horn of the spinal cord.

The Pearson linear correlation coefficient (r) was used to measure the degree of intensity of the correlation between 2 variables. It is known that this coefficient must be 0.6 or more to permit reaching a conclusion. Below this value, the correlation between variables is weak.

RESULTS

Nerve Loops

There was communication between the stump and the region of end-to-side neurorrhaphy. Because this communication was shaped as an arch, we opted to define it as a nerve loop and not simply as a contamination loop. These nerve loops were detected in 3 animals submitted to end-to-side neurorrhaphy, both with and without an epineurial window, and their morphometric analysis revealed the presence of numerous nerve fibers (Fig. 3).

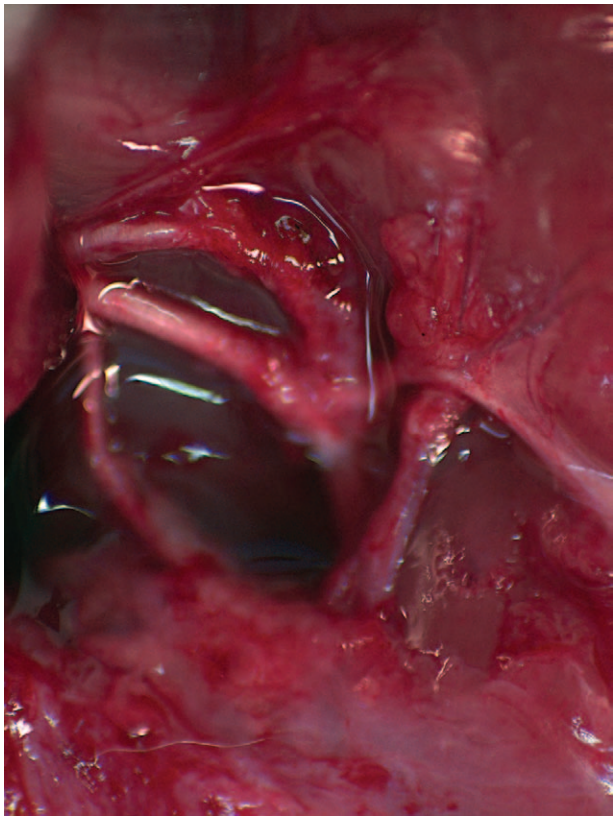

Fig. 3. Example of intraoperative nerve loop.

Morphometry Data

The mean number of fibular nerve fibers was significantly higher in the positive control group compared to the tested groups (Fig. 4), as determined by the ANOVA option of the Graphpad Instat software ($P = 0.0002$).

There was no difference between the positive control group (end-to-end neurorrhaphy) and the negative control group (sham) ($q = 0.6340$ and $P > 0.05$). However, the mean number of fibers was significantly higher in the positive control group compared with the end-to-side neurorrhaphy groups ($q = 5.243$ and $P < 0.01$) in the presence of an epineurial window and ($q = 4.951$ and $P < 0.01$) in the absence of an epineurial window (See **Supplemental Digital Content 1**, which displays distribution of the mean number of regenerated fibers in the fibular nerve different between the groups, ***http://links.lww.com/PRSGO/A87***).

Electron Microscopy

ANOVA of the fiber perimeter between groups showed that the perimeter was significantly greater in the sham and end-to-end neurorrhaphy groups when compared with the end-to-side neurorrhaphy groups with and without an epineurial window (Figs. 5–8). The mean nerve fiber perimeter did not differ significantly between the sham and positive control groups.

HRP Labeling

Mean HRP labeling in the anterior horn of the spinal cord did not differ significantly between the negative control group (sham) and the positive control group (end-to-end neurorrhaphy) ($q = 0.6647$ and $P > 0.05$). However, neuronal HRP labeling was significantly higher in the anterior horn of the spinal cord of the positive control group (end-to-end neurorrhaphy) than in the groups submitted to end-to-side neurorrhaphy with an epineurial window ($q = 5.291$ and $P < 0.01$) and without an epineurial window ($q = 5.617$ and $P < 0.01$) (Figs. 9–12). Finally, comparison of the end-to-side neurorrhaphy groups with and without an epineurial window revealed no significant difference ($q = 0.3489$ and $P > 0.05$) (See **Supplemental Digital Content 2**, which displays distribution of the neuronal HRP labeling in the anterior horn of the spinal cord evaluated between the groups, ***http://links.lww.com/PRSGO/A88***).

The animals submitted to HRP analysis in the right lower limb acted as their own controls. The left lower limb was injected with HRP in the fibular muscles but was not operated on. The results showed no difference in mean HRP labeling in the left anterior horn of the spinal cord between groups.

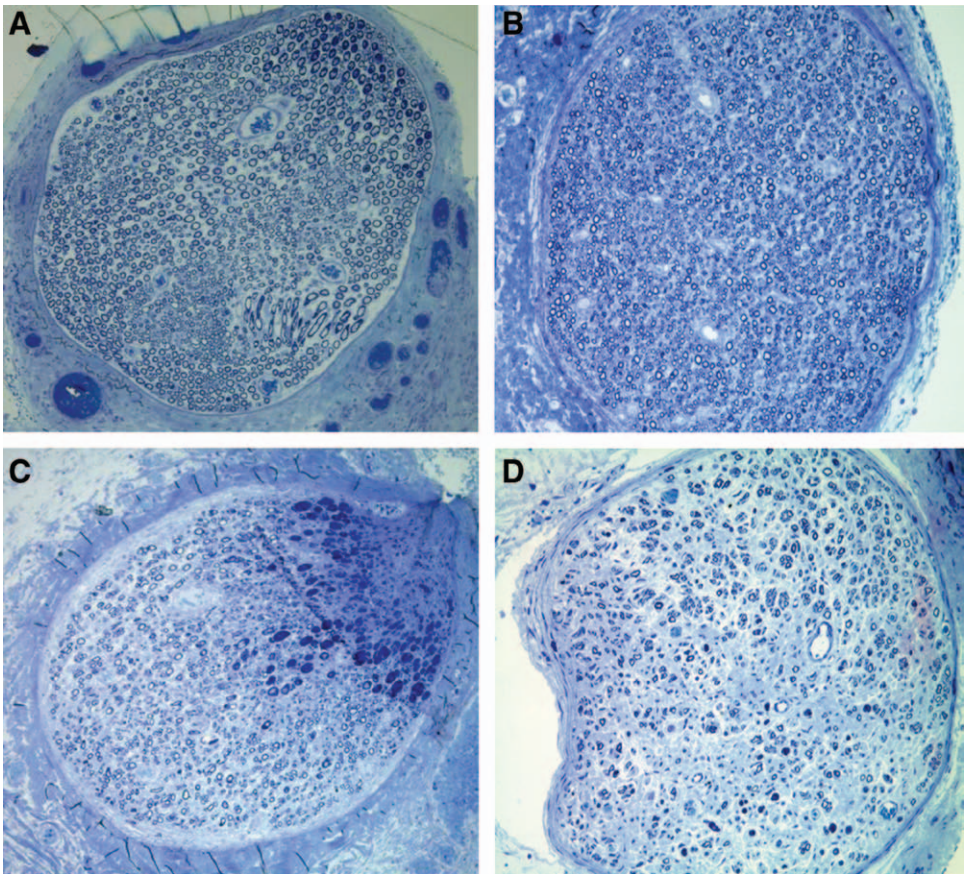

Fig. 4. Cross section of the peroneal nerve regeneration (1% toluidine blue). A, Sham group. B, End-to-end neurorrhaphy. C, End-to-side neurorrhaphy with epineural window. D, End-to-side neurorrhaphy without epineural window.

FG Labeling

The mean areas labeled with FG in the anterior horn of the spinal cord did not differ significantly between the negative control group (sham) and the positive control group (end-to-end neurorrhaphy) ($q = 0.2346$ and $P > 0.05$) (Figs. 13–16). Conversely,

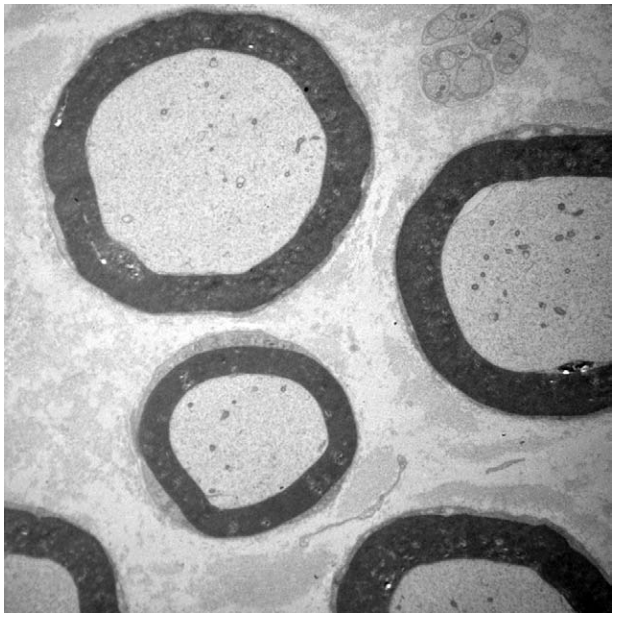

Fig. 5. Electron micrograph of the peroneal nerve with myelin fibers (×5000)—sham group.

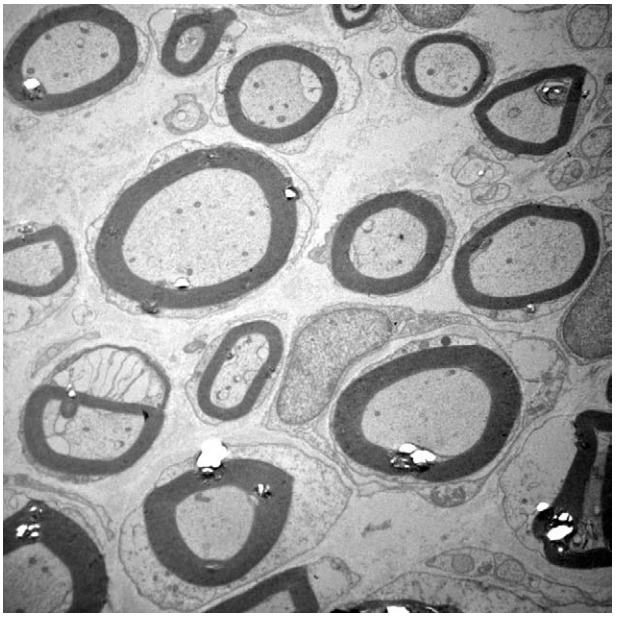

Fig. 6. Electron micrograph of the peroneal nerve with myelin fibers (×5000)—end-to-end neurorrhaphy group.

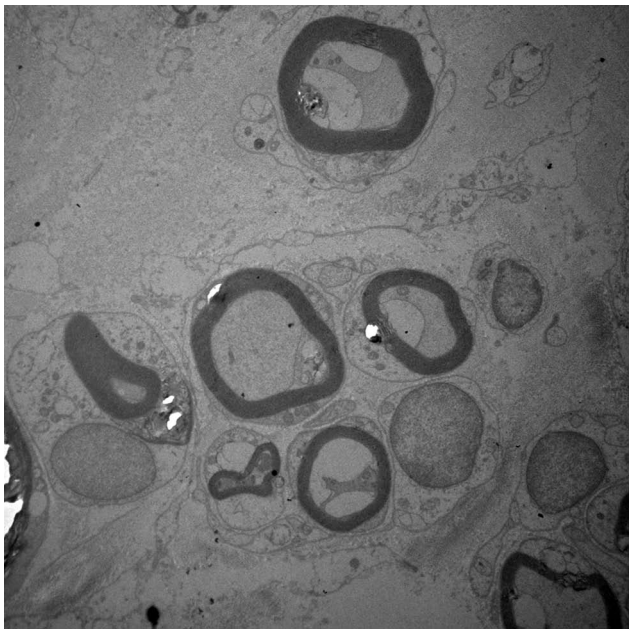

Fig. 7. Electron micrograph of the peroneal nerve with myelin fibers (×5000)—end-to-side neurorrhaphy with epineural window.

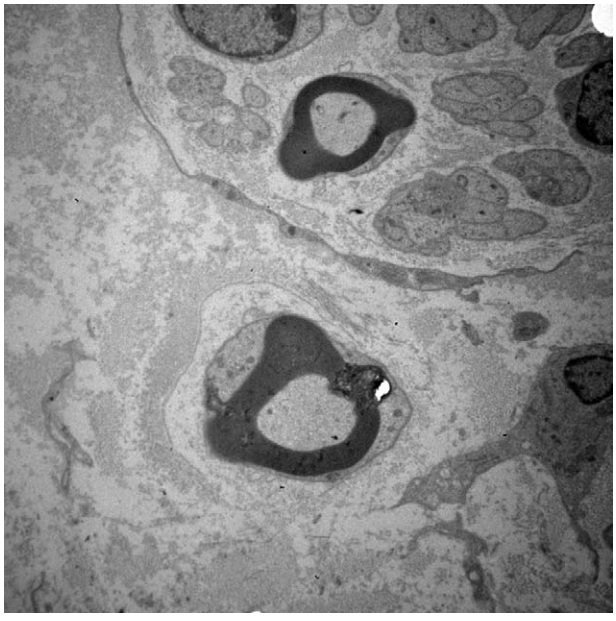

Fig. 8. Electron micrograph of the peroneal nerve with myelin fibers (×5000)—end-to-side neurorrhaphy without epineural window.

there was a significant difference in the mean FG-labeled areas between the positive control group (end-to-end neurorrhaphy) and the end-to-side neurorrhaphy group with an epineural window ($q = 4.071$ and $P < 0.05$) and the end-to-side neurorrhaphy group without an epineurial window ($q = 4.08$ and $P < 0.05$) (See **Supplemental Digital Content 3**, which displays mean areas labeled with FG in the anterior horn of the spinal cord differing between the groups, ***http://links.lww.com/PRSGO/A89***).

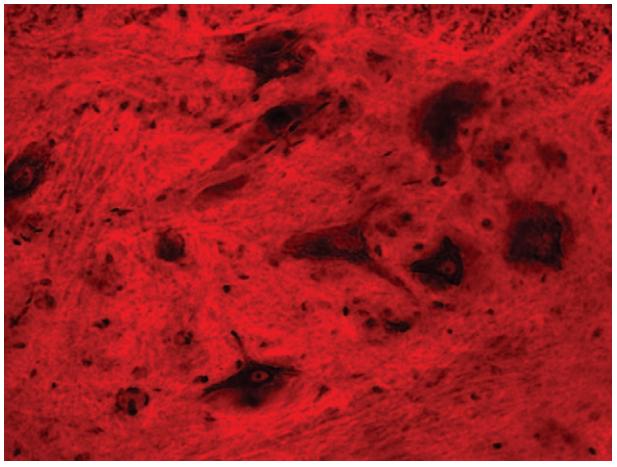

Fig. 9. Cross section of the spinal cord showing motor neurons of the animal marked with HRP (×40 magnification—sham group).

Electroneuromyography

The objective was to compare the amplitudes of the action potentials in the fibular muscles. No significant difference was detected between the positive control group (end-to-end neurorrhaphy) and the negative control group (sham) ($q = 1.661$ and $P > 0.05$, respectively). However, there was a significant difference between the positive control (end-to-end neurorrhaphy) and the end-to-side neurorrhaphy group with and without an epineurial window ($q = 3.935$ and $P < 0.05$ and $q = 4.029$ and $P < 0.05$, respectively).

The amplitudes of the action potentials generated in the electroneuromyography examination were significantly greater in the sham and end-to-

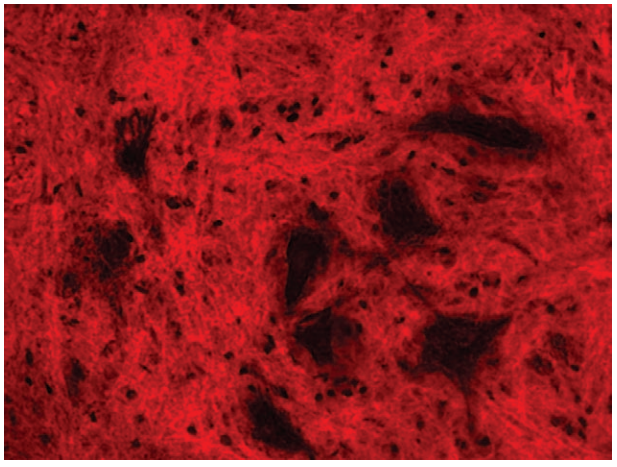

Fig. 10. Cross section of the spinal cord showing motor neurons of the animal marked with HRP (×40 magnification—end-to-end neurorrhaphy group).

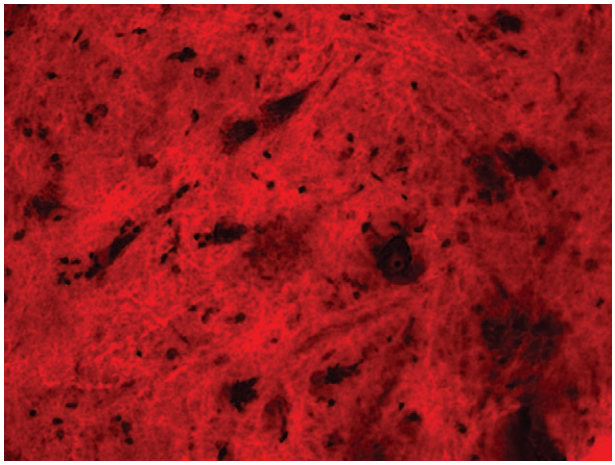

Fig. 11. Cross section of the spinal cord showing motor neurons of the animal marked with HRP (×40 magnification—end-to-side neurorrhaphy with epineural window group).

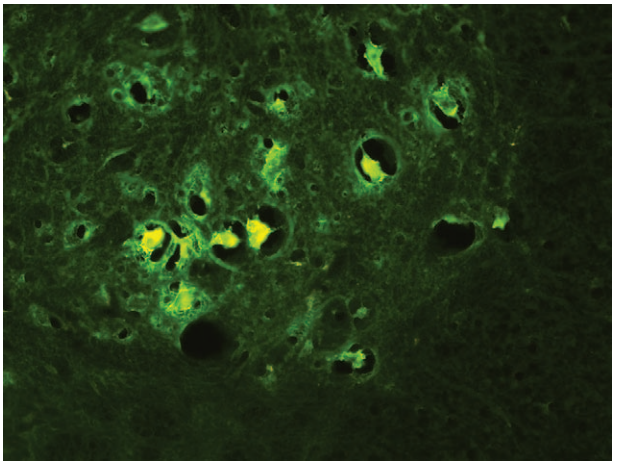

Fig. 13. Cross section of the gray matter of the spinal cord showing motor neurons of the FG-labeled animal (×20 magnification—sham group).

end neurorrhaphy groups than in the remaining groups, indirectly revealing the contingent of axons in the nerve under study (See **Supplemental Digital Content 4**, which displays distribution of electrophysiological motor unit potentials in the groups evaluated after nerve regeneration, ***http://links.lww.com/PRSGO/A90***).

By contrast, the variations between groups in the mean electroneuromyographic amplitudes in the left (nonoperated) lower limbs were not greater than expected by chance. However, the variation in mean electroneuromyographic latencies between the groups studied was not significantly higher than expected by chance. A possible explanation for the absence of differences in latency between groups was the presence of some thick fibers (more than 7 μm in diameter) in the group of end-to-side neurorrhaphy with (4%) and without (3%) an epineurial window.

Result of Linear Regression

The Pearson correlation coefficient between HRP-labeled neurons in the anterior horn of the spinal cord and fiber count after end-to-end neurorrhaphy was 0.85 (>0.6), considered to be a strong value (Fig. 17).

The coefficient of determination between HRP-labeled neurons and fiber count after end-to-end neurorrhaphy was 73%, that is, in 73% of cases the changes in neuronal labeling with HRP caused changes in fiber count after end-to-end neurorrhaphy.

DISCUSSION

Several authors have demonstrated that nerve regeneration after end-to-side neurorrhaphy occurs through contact of the recipient nerve with the donor nerve and that after this contact there is a disintegration of the layers wrapping the nerve for axonal growth, with no harm to the donor nerve.[3-5,8,9]

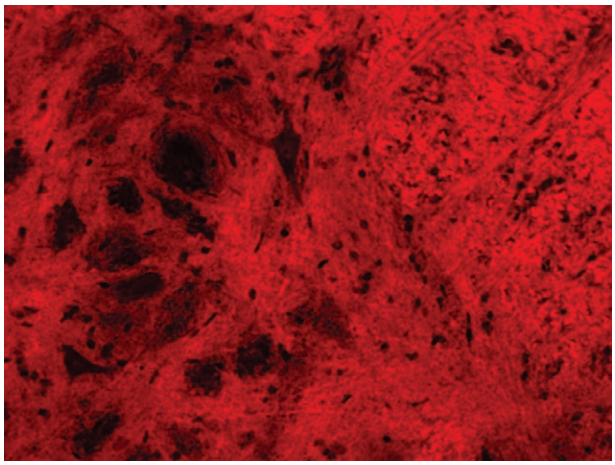

Fig. 12. Cross section of the spinal cord showing motor neurons of the animal marked with HRP (×40 magnification—end-to-side neurorrhaphy without epineural window group).

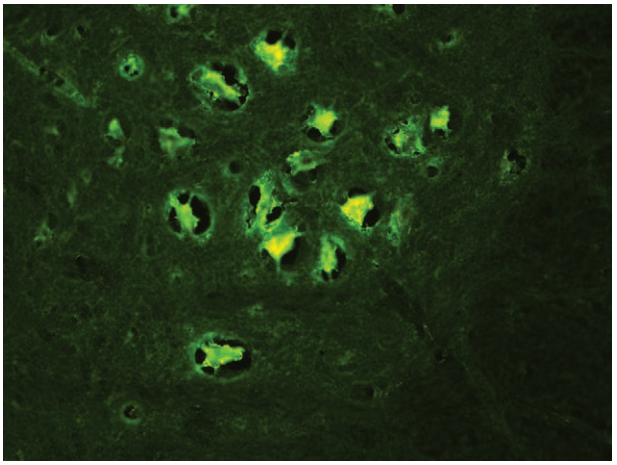

Fig. 14. Cross section of the gray matter of the spinal cord showing motor neurons of the FG-labeled animal (×20 magnification—end-to-end neurorrhaphy).

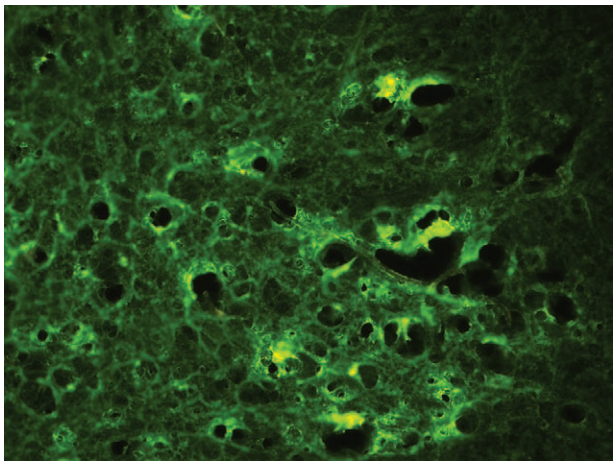

Fig. 15. Cross section of the gray matter of the spinal cord showing motor neurons of the FG-labeled animal (×20 magnification—end-to-side neurorrhaphy with epineural window).

According to some investigators, the accepted mechanism of regeneration after end-to-side neurorrhaphy is collateral axon sprouting from the closest Ranver nodes on the side of the anastomosis. This mechanism starts by the action of factors released by Schwann cells and fibroblasts.

Additionally, other investigators believe that the epineurial window is essential for sprouting because its absence would not permit the intact nerve to transmit axons that would transpose the epineurium.[10,11] Others[12,13] consider the layers of the peripheral nerve to be barriers against axon penetration during regeneration and do not recommend this technique for clinical use.

An interesting fact observed in the present study was the identification of a nerve loop between the proximal stump of the fibular nerve and the anastomosis region in groups 3 and 4, even when it was fixed to the adjacent muscles with 8-0 mononylon suture, a fact contributing to the explanation of nerve regeneration after end-to-side neurorrhaphy (groups 3 and 4). These loop segments were sectioned and submitted to morphometric analysis, which identified nerve fibers. Thus, we suggest that these loops contributed to the regeneration of the fibular nerve. Because this loop was not identified in all cases, we suggest that collateral sprouting was induced by neural contact in association with the stimulus of the passage of the stitch and the epineural window, contributing to regeneration in other cases.

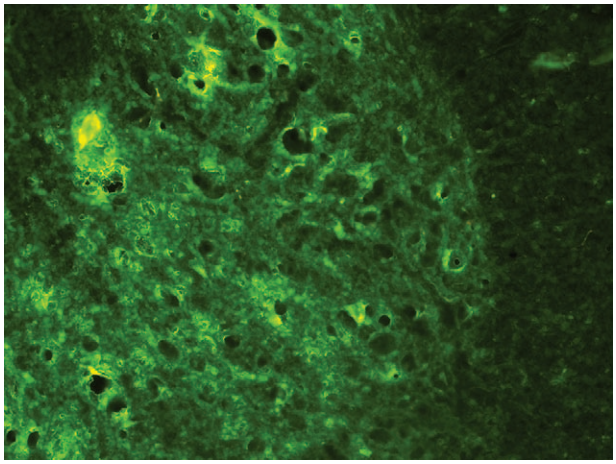

Fig. 16. Cross section of the gray matter of the spinal cord showing motor neurons of the FG-labeled animal (×20 magnification—end-to-side neurorrhaphy without epineural window).

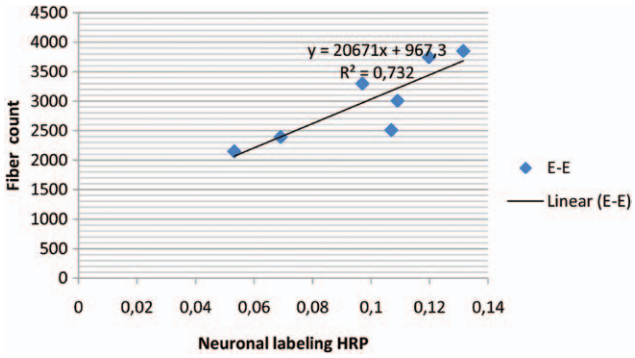

Fig. 17. Relationship between neuronal labeling by HRP and the count of nerve fibers in the peroneal nerve after end-to-end neurorrhaphy.

In addition, nerve regeneration was also assessed by neurotracer uptake in the axon endings and by its identification in the anterior horn of the spinal cord.

Labeling of the cell bodies in the anterior horn of the spinal cord was detected in all operated animals that received an HRP injection in the fibular muscle. This implied that the number of motor neurons in the anterior horn of the spinal cord was similar to that of the sham group and was significantly higher than that of the group with end-to-side neurorrhaphy with or without an epineurial window. To contribute to this evaluation, the left lower limb, which received an HRP injection but was not operated upon, was analyzed, and the result on this side did not show a significant difference.

Neuronal FG uptake was assessed in 20 other animals and showed similar results. On the basis of the number of motor neurons labeled with FG in the ventral horn of the spinal cord, we demonstrated the preservation of a larger number of motor neurons after end-to-end neurorrhaphy compared with the other groups. In other words, there was a higher rate of cell death in the fibular nerve cord in the end-to-side neurorrhaphy group.

Both HRP and FG were useful for the assessment of nerve regeneration in the groups studied.

The present study showed a statistically significant correlation between neuronal labeling in the ventral horn of the spinal cord and fiber count after end-to-end neurorrhaphy. The coefficient of determination between HRP-labeled neurons and fiber count was 73% after end-to-end neurorrhaphy, that is, in 73% of cases the changes in neuronal labeling with HRP caused alterations in fiber count after end-to-end neurorrhaphy. We observed that, after end-to-end neurorrhaphy, the fiber count increased linearly with increasing number of HRP-labeled neurons.

CONCLUSIONS

We conclude that nerve regeneration occurred in all groups studied, as determined by morphometry, electroneuromyography, and neuronal uptake of the neurotracer. However, significantly better results were obtained for the end-to-end neurorrhaphy group than for the groups submitted to end-to-side neurorrhaphy with or without an epineurial window. Particularly noteworthy was the identification of a nerve loop in groups 3 and 4, which contributed to the regeneration of the distal stump of the fibular nerve.

Carlos Eduardo Fagotti de Almeida, MD, PhD
Division of Plastic Surgery
Department of Surgery and Anatomy
Ribeirão Preto Medical School
University of São Paulo
Avenida Bandeirantes 3900
9° andar, CEP 14048–900
Ribeirão Preto SP, Brazil
E-mail: cefagotti@gmail.com

REFERENCES

1. Kristensson K, Olsson Y. Retrograde axonal transport of protein. *Brain Res.* 1971;29:363–365.
2. Schmued LC, Fallon JH. Fluoro-Gold: a new fluorescent retrograde axonal tracer with numerous unique properties. *Brain Res.* 1986;377:147–154.
3. Viterbo F, Trindade JC, Hoshino K, et al. Latero-terminal neurorrhaphy without removal of the epineural sheath. Experimental study in rats. *Rev Paul Med.* 1992;110: 267–275.
4. Viterbo F, Trindade JC, Hoshino K, et al. Two end-to-side neurorrhaphies and nerve graft with removal of the epineural sheath: experimental study in rats. *Br J Plast Surg.* 1994;47:75–80.
5. Viterbo F, Trindade JC, Hoshino K, et al. End-to-side neurorrhaphy with removal of the epineurial sheath: an experimental study in rats. *Plast Reconstr Surg.* 1994;94:1038–1047.
6. Terzis JK, Fortes WM, Linzzi F, et al. End-to-side neurorrhaphy: evaluation of nerve growth factor elaboration using cRNA probes (in situ hybridization). *J Reconstr Microsurg.* 1997;13:136.
7. Bertelli JA, Ghizoni MF. Nerve repair by end-to-side coaptation or fascicular transfer: a clinical study. *J Reconstr Microsurg.* 2003;19:313–318.
8. Viterbo F, Teixeira E, Hoshino K, et al. End-to-side neurorrhaphy with and without perineurium. *Sao Paulo Med J.* 1998;116:1808–1814.
9. Zhang F, Cheng C, Chin BT, et al. Results of terminolateral neurorrhaphy to original and adjacent nerves. *Microsurgery* 1998;18:276–281.
10. McCallister WV, Tang P, Trumble TE. Is end-to-side neurorrhaphy effective? A study of axonal sprouting stimulated from intact nerves. *J Reconstr Microsurg.* 1999;15:597–603; discussion 603–604.
11. Rovak JM, Cederna PS, Kuzon WM Jr. Terminolateral neurorrhaphy: a review of the literature. *J Reconstr Microsurg.* 2001;17:615–624.
12. Bertelli JA, dos Santos AR, Calixto JB. Is axonal sprouting able to traverse the conjunctival layers of the peripheral nerve? A behavioral, motor, and sensory study of end-to-side nerve anastomosis. *J Reconstr Microsurg.* 1996;12: 559–563.
13. Pannucci C, Myckatyn TM, Mackinnon SE, et al. End-to-side nerve repair: review of the literature. *Restor Neurol Neurosci.* 2007;25:45–63.